frontiers in Sustainable Food Systems

ORIGINAL RESEARCH
published: 30 March 2022
doi: 10.3389/fsufs.2022.844485

The Improvement of the Modified Starch—Glucomannan—Polyvinyl Alcohol Biothermoplastic Composite Characteristics With Polycaprolactone and Anhydride Maleic Acid

Bambang Admadi Harsojuwono [1], I. Wayan Arnata [1], Amna Hartiati [1], Yohanes Setiyo [2], Sayi Hatiningsih [3] and Luh Suriati [4]*

[1] Agroindustry Technology Department, Agriculture Technology Faculty, Udayana Uiversity, Jimbaran, Indonesia, [2] Engineering and Bio System Department, Agriculture Technology Faculty, Udayana University, Jimbaran, Indonesia, [3] Food Science and Technology Department, Agriculture Technology Faculty, Udayana University, Jimbaran, Indonesia, [4] Food Technology Department, Agriculture Faculty, Warmadewa University, Denpasar, Indonesia

OPEN ACCESS

Edited by:
Danar Praseptiangga, Sebelas Maret University, Indonesia

Reviewed by:
Saiful Irwan Zubairi, National University of Malaysia, Malaysia
Asad Mohammad Amini, University of Kurdistan, Iran

***Correspondence:**
Bambang Admadi Harsojuwono
bambang.admadi@unud.ac.id

Specialty section:
This article was submitted to Sustainable Food Processing, a section of the journal Frontiers in Sustainable Food Systems

Received: *28 December 2021*
Accepted: *28 January 2022*
Published: *30 March 2022*

Citation:
Harsojuwono BA, Arnata IW, Hartiati A, Setiyo Y, Hatiningsih S and Suriati L (2022) The Improvement of the Modified Starch—Glucomannan—Polyvinyl Alcohol Biothermoplastic Composite Characteristics With Polycaprolactone and Anhydride Maleic Acid. Front. Sustain. Food Syst. 6:844485. doi: 10.3389/fsufs.2022.844485

The purpose of this study was to determine the concentrations of polycaprolactone (PCL) and anhydride maleic acid (AMA) to produce a biothermoplastic composite (BtC) of modified cassava starch–glucomannan–polyvinyl alcohol (MSGPvA) that meets the Indonesian National Standard (SNI) and International Bioplastic Standards such as ISO 527/1B, PCL from the UK, and ASTM 5336 for PLA plastic from Japan. This study measured the tensile strength ratio and Young's modulus of MSGPvA BtC compared to commercial biothermoplastic (CBt), elongation at break, swelling, water vapor transmission rate (WVTR), and biodegradation time. In addition, the surface profile, functional group, crystallinity, and thermal stability were also observed, which were analyzed qualitatively and quantitatively. MSGPvA BtC with 20% PCL and 3.5% AMA was able to increase and improve tensile strength, elongation at break, Young's modulus, swelling, WVTR, and degradation time. MSGPvA BtC with 5% PCL and 0.5% AMA has a transverse surface profile that shows the presence of clear and wavy fibers and an elongated surface profile with indistinct waves, containing the OH functional group at wavenumbers 2,962.66 and 3,448.72 cm^{-1} and C=O at a wavenumber of 1,735.93 cm^{-1}, and has a low crystallinity degree but relatively high thermal stability. All MSGPvA BtC characteristics with 5% PCL and 0.5% AMA have met the SNI and International Bioplastic Standards (ISO 527/1B, PCL from England, ASTM 5336 for PLA plastic from Japan), except for swelling characteristics. Thus, MSGPvA BtC with 5% PCL and 0.5% AMA has the potential to be used as food packaging material.

Keywords: modified starch, glucomannan, polyvinyl alcohol, polycaprolactone, anhydride maleic acid

INTRODUCTION

Plastic has become an environmental problem because the waste is difficult to decompose in the soil and burning it can be toxic. Therefore, it is necessary to develop alternative products that are environmentally friendly such as bioplastics. One example of bioplastics that has become a future trend and has begun to be widely studied is biothermoplastic composite (BtC). Potential biological natural materials as raw materials for BtC are cassava starch and glucomannan (Harsojuwono and Arnata, 2016). According to Firdaus and Anwar (2014), both are mass-produced and renewable so that their availability is guaranteed. Several studies have been carried out such as that by Abdurrozag (2016) who made a bioplastic composite from a mixture of 30% glucomannan and 70% starch with 25% glycerol as a plasticizer, having a tensile strength of 9.3 MPa, elongation at break of 44.68%, swelling of 136.73%, and degradation time of 20.5 days. Meanwhile, Harsojuwono et al. (2021) have developed a BtC from modified cassava starch, glucomannan, and polyvinyl alcohol (MSGPvA), which has the characteristics of being able to melt and stick with a tensile strength value 1.1 times that of commercial biothermoplastic (CBt), elongation at break of 8.10%, Young's modulus 1.12 times that from CBt, swelling of 10.72%, and biodegradation time of 5.25 days. The results obtained show that not all of the characteristics meet the Indonesian National Standard (SNI), an international plastic standards (ISO 527/1B, PCL from the UK, ASTM 5336 for PLA plastic from Japan). Therefore, it is necessary to improve and develop MSGPvA BtC.

Many factors influence the manufacture of BtC such as the type and concentration of plasticizer (Dewi et al., 2015), the concentration of polymeric materials (Harsojuwono and Arnata, 2016), temperature and drying time (Harsojuwono et al., 2017), gelatinization temperature and pH (Harsojuwono et al., 2018), polymer mixture ratio and solvent concentration (Harsojuwono et al., 2019), filler type and concentration (Harsojuwono et al., 2020), the use of coupling agents (Melani et al., 2017), reinforcing materials (Dewi et al., 2015), and compatibilizer (Waryat et al., 2018).

One of the efforts is to add hydrophobic biodegradable reinforcing materials such as polycaprolactone (PCL). Carballo et al. (2017) showed that a mixture of thermoplastic starch and PCL had better water resistance than one without PCL. Biocompatible PCL when added to resin can improve mechanical properties, biodegradability, flexibility, and resistance to water (Warastuti et al., 2017; Anonymous, 2020). PCL mixed with polylactic acid had no detrimental effect on the softening and melting temperature of the composite (Ryden et al., 2016). According to Chen and Sun (2005) and Warastuti et al. (2017), the use of PCL 20–25% w/w of the total polymer material produces an applicable composite. However, the excess of PCL will not be beneficial if hydrophilic MSGPvA is mixed with hydrophobic PCL, because both cannot be completely mixed. Therefore, it is necessary to have a compatibilizer material such as anhydride maleic acid (AMA), which is the link between hydrophilic and hydrophobic components, so as to increase adhesion and decrease the surface tension of the two different materials (Prachayawarakorn et al., 2010; Pushpadass et al., 2010; Waryat et al., 2018). Muin (2019) showed that copolymerization of laboplastomil and LLDPE using AMA was able to increase 28% tensile strength, 99% boiling point, 203% elongation at break, and 163% crystallinity compared to pure LLDPE. The higher the concentration of AMA between 1.5 and 5.0% w/w of the polymer material, the higher the Young modulus of the polypropylene/montmorillonite nanocomposite (Akbari and Bagheri, 2012).

The description above shows that there is no information on the use of PCL and AMA with various concentrations in the manufacture of MSGPvA BtC. Therefore, it is necessary to investigate the use of appropriate concentrations of PCL and AMA in the manufacture of MSGPvA BtC in order to produce products that have better water resistance and meet the International Plastic Standards and SNI.

The purpose of this study was to determine the effect of the concentration of PCL, AMA, and their interactions on the characteristics of MSGPvA BtC and to determine the concentration of PCL and AMA to produce MSGPvA BtC that meets SNI and International Bioplastic Standards.

MATERIALS AND METHODS

Materials

The research materials were the modified cassava starch, glucomannan (konjac glucomannan) from CV Nura Jaya; distilled water, acetic acid, ZnO, and glycerol from CV Saba Kimia; and polyvinyl alcohol (PVA), PCL, and AMA from CV Duta Jaya.

Experimental Designs

The experimental design in this study was a factorial randomized block design. Factor I is the concentration of PCL with four levels, namely 5, 10, 15, and 20% w/w of the total polymer material. Factor II is the concentration of AMA with four levels, namely, 0.5, 1.5, 2.5, and 3.5% w/w of the total polymer material. The experiment has 16 combination treatments grouped into three manufacturing processes of the BtC with 48 experimental units.

Research Implementation

Cassava starch and glucomannan in a ratio of 3:1 was modified with an amount of 6 g plus 90 g 1% acetic acid solution, then heated in a water bath at 75 + 1°C, and stirred using a lab mixer at 60 rpm to form a gel. The heated gel was added with 1 g of glycerol, 0.6 g of ZnO, and 3 g of PVA and then stirred using a lab mixer at 60 rpm in a water bath for 5 min at a temperature of 75 + 1°C. Then PCL gel (PCL was dissolved and stirred in ethyl acetate in a ratio of 1:1) and AMA with the appropriate concentration were added over a water bath at 75 + 1°C and stirred using a lab mixer at 60 rpm for 5 min. The gel was molded in a Teflon mold with a diameter of 20 cm and then dried in a drying oven at 60°C for 5 h. The BtC formed was cooled at room temperature and then removed from the Teflon mold after 24 h (Harsojuwono et al., 2020).

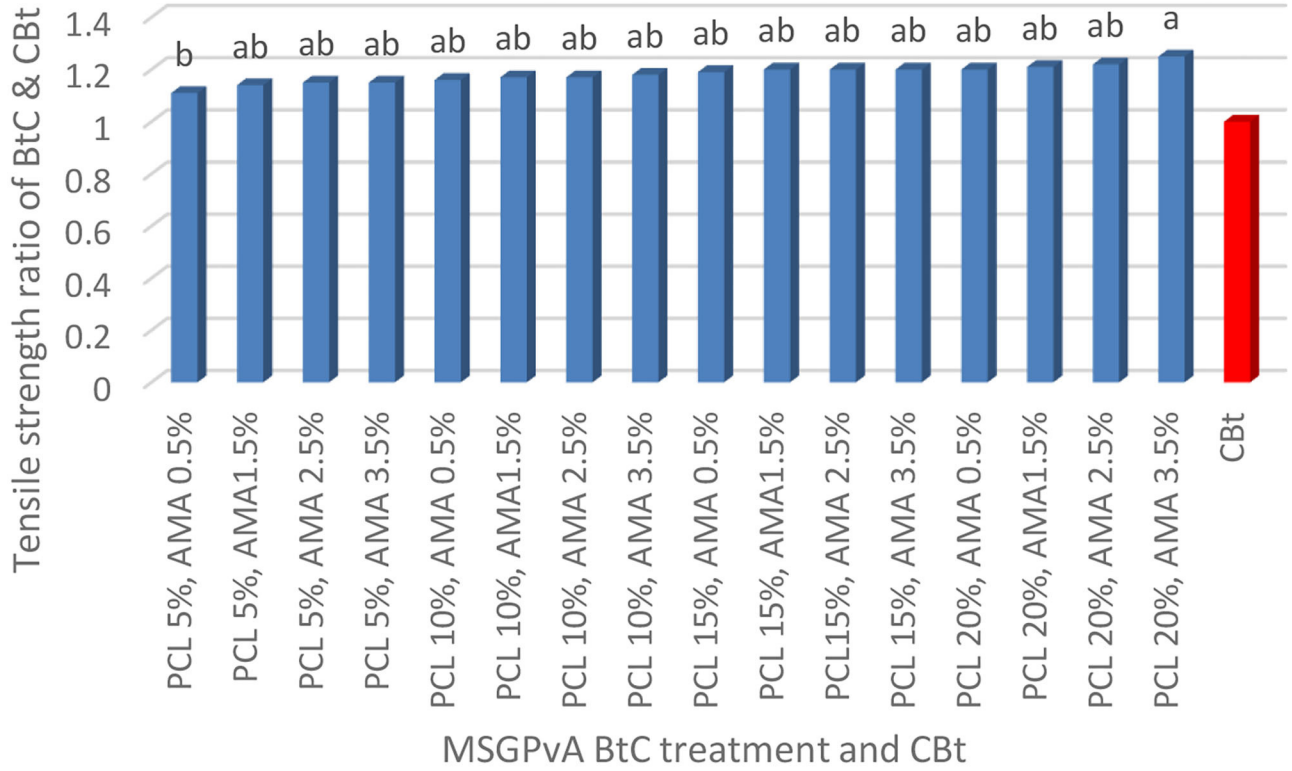

FIGURE 1 | Relationship of MSGPvA BtC and CBt with the tensile strength ratio of BtC to CBt.

Observation Variable

A mechanical test (ASTM D638) was performed, consisting of the tensile strength ratio of BtC to CBt with brand TB, elongation at break, Young's modulus ratio of BtC to CBt, swelling, water vapor transmission rate (WVTR), biodegradation time (ISO 17556), surface profile using SEM Zeiss EVO MA10 (Harsojuwono and Arnata, 2017), functional groups using the FTIR spectrometer Bruker-Tensor 37 (Gable, 2014), crystallinity using X-ray Diffractometer Bruker Advance D8 (Sharma et al., 2012), and thermal stability using TG/DTA Shimadzu DTG-60 Series Differential Thermal-Thermogravimetric Analyzer (Hestuti et al., 2017).

Data Analysis

The ratio of tensile strength, elongation at break, ratio of Young's modulus, swelling, WVTR, and biodegradation time were analyzed by ANOVA and followed by the Duncan multiple range test using the SPSS 25 program. Meanwhile, the data from surface profile variables, functional groups, crystallinity, and thermal stability were analyzed in a descriptive-qualitative and quantitative method.

RESULTS AND DISCUSSION

Tensile Strength, Elongation at Break, and Young's Modulus

The concentration of PCL and AMA and their interactions had a very significant effect on elongation at break and the ratio of tensile strength and Young's modulus of MSGPvA BtC to CBt. The tensile strength ratio range of MSGPvA BtC to CBt is between 1.11 ± 0.02 and 1.25 ± 0.01 (**Figure 1**), elongation at break ranges from 8.01 ± 0.01 to 10.67 ± 0.03% (**Figure 2**), and Young's modulus ratio ranges from 1.13 ± 0.01 to 1.36 ± 0.01 (**Figure 3**).

Figure 1 shows that the MSGPvA BtC using 20% PCL and 3.5% AMA had the highest tensile strength with a value 1.25 ± 0.01 times that of CBt, which was not significantly different from the tensile strength values of the MSGPvA BtC with all PCL and AMA treatments, except for the MSGPvA BtC which uses 5% PCL with 0.5% AMA, which is 1.11 ± 0.02 times the tensile strength of CBt. This value is the lowest tensile strength of the MSGPvA BtC using PCL and AMA.

MSGPvA BtC using 20% PCL and 3.5% AMA has a tensile strength value that is 1.25 + 0.01 times that of CBt; this value is higher than the tensile strength of MSGPvA BtC from Harsojuwono et al. (2021). According to Frost et al. (2009) and Dome et al. (2020), tensile strength is strongly influenced by the presence of a mixture of other materials and the crystallinity degree of the material.

It was further explained that the presence of double- and single-helical structures in polysaccharides greatly determines the degree of crystallinity so that it affects the tensile strength. The MSGPvA BtC using 20% PCL and 3.5% AMA has met the biothermoplastic standard SNI 7818:2014, which sets a tensile strength value of 24.7–302 MPa; the international bioplastic standard ISO 527/1B, which sets a tensile strength value of 35.95

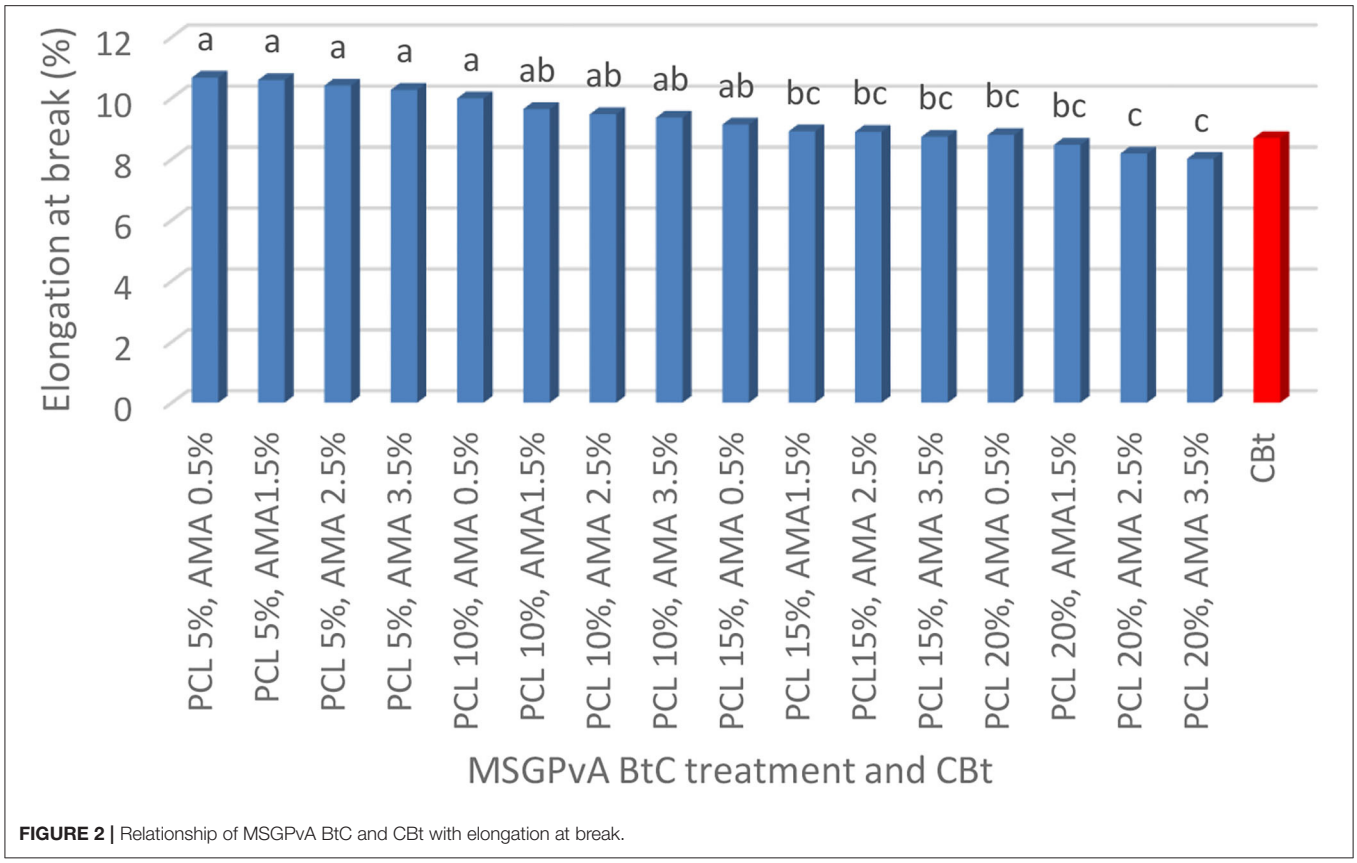

FIGURE 2 | Relationship of MSGPvA BtC and CBt with elongation at break.

MPa, PCL from the UK, which sets a tensile strength value of at least 190 MPa; and ASTM 5336 for PLA plastic from Japan, which sets a tensile strength value of 2,050 MPa (Averous, 2007).

Figure 2 also shows that the MSGPvA BtC using 20% PCL and 2.5–3.5% AMA has a low elongation at break (8.01 ± 0.04%—8.19 ± 0.05%) and is not significantly different from the elongation at break of the MSGPvA BtC using 15% PCL with 1.5–3.5% AMA and 20% PCL with 1.5% AMA. Meanwhile, the MSGPvA BtC using 5% PCL with 0.5–3.5% AMA and 10% PCL with 0.5% AMA had a high elongation at break and was not significantly different from the elongation at break of the MSGPvA BtC which used 10% PCL with 1.5–3.5% AMA and 15% PCL with 0.5% AMA.

The MSGPvA BtC with 20% PCL and 2.5–3.5% AMA had an elongation at a break value of 8.01 ± 0.04%—8.19 ± 0.05%. This value is similar to that of MSGPvA with an elongation at a break of 8.10 ± 0.03% (Harsojuwono et al., 2021). There are variations in elongation at break due to differences in macrostructure and microstructure of bioplastic composites (Nayiroh, 2013). According to Harsojuwono and Arnata (2017), macrostructure and microstructure are influenced by the degree of crystallinity. According to Zhong and Kang (2008), elongation at break that is too high or too low occurs due to disruption of compatibility and homogeneity, resulting in an imbalance of functional groups due to the ratio of material concentration and process temperature that is too extreme, which results in molecular dispersion that affects mechanical properties including elongation at break. The MSGPvA BtC with 20% PCL and 2.5–3.5% AMA has an elongation-at-break value in accordance with the PLA plastic standard from Japan (maximum elongation-at-break value of 9%). Meanwhile, all MSGPvA BtCs have an elongation-at-break value in accordance with the PCL plastics standard from the UK (maximum elongation-at-break value of 500%).

Figure 3 also shows that the MSGPvA BtC using 20% PCL and 2.5–3.5% AMA has high Young's modulus (1.35 ± 0.02–1.36 ± 0.02 times that of the CBt Young's modulus), which is significantly different from Young's modulus of MSGPvA BtC using 5% PCL and 0.5–3.5% AMA. Meanwhile, the MSGPvA BtC using 5% PCL and 0.5% AMA had the lowest Young's modulus value and was not significantly different from Young's modulus of the MSGPvA BtC using 5% PCL and 1.5–3.5% AMA.

The MSGPvA BtC with 20% PCL and 3.5% AMA had a Young's modulus 1.36 times that of the CBt Young modulus, which was higher than Young's modulus of MSGPvA from Harsojuwono et al. (2021). Basically, Young's modulus is the ability of a material to return to its original shape when stressed; therefore, Young's modulus is highly dependent on tensile strength and elongation at break (Tong et al., 2017).

Thus, it is strongly influenced by the macrostructure and microstructure of the polymer (Nayiroh, 2013), such as the degree of crystallinity, the degree of cross-linking, the value of the glass transition point and melting point, molecular mass, and polydispersity or molecular mass distribution (Harsojuwono and

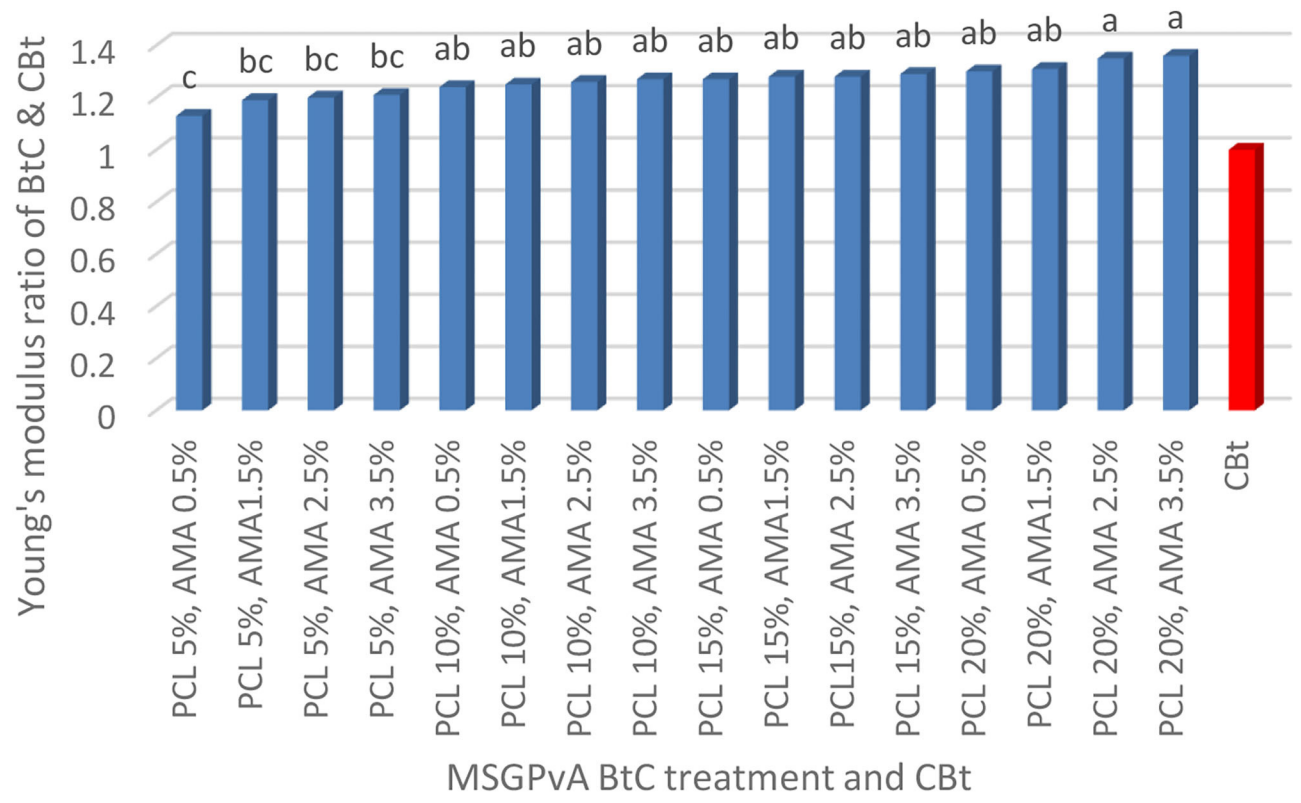

FIGURE 3 | Relationship of MSGPvA BtC and CBT with Young's modulus ratio of BtC to CBt.

Arnata, 2017). Meanwhile, all MSGPvA BtC using PCL and AMA have met the ISO 527/1B international plastic standard with a minimum Young's modulus value of 6.019 MPa.

Swelling, WVTR, and Biodegradation Time

The concentration of PCL and AMA and their interactions had a very significant effect on swelling and WVTR, but it did not affect the degradation time of the MSGPvA BtC. The swelling range value is between 4.85 ± 0.03% and 10.06 ± 0.05% (**Figure 4**), WVTR is between 91.12 ± 0.81 and 167.89 ± 1.05 g/m^2/day (**Figure 5**), and the degradation time is between 6.33 ± 0.03 and 7.33 ± 0.02 days (**Figure 6**).

Figure 4 shows that the MSGPvA BtC using 5% PCL and 0.5–2.5% AMA had a high swelling value (9.07 ± 0.03%−10.06 ± 0.05%), which was not significantly different from the swelling of the MSGPvA BtC using 5% PCL with 3.5% AMA and 10% PCL with 0.5–1.5% AMA. Meanwhile, the MSGPvA BtC using 20% PCL and 1.5–3.5% AMA had a low swelling value (4.85 ± 0.03%−5.45 ± 0.01%), which was not significantly different from the swelling value of the MSGPvA BtC using 10% PCL and 2.5–3.5% AMA, 15% PCL and 0.5–3.5% AMA, and 20% PCL and 3.5% AMA.

The MSGPvA BtC with 20% PCL and 1.5–3.5% AMA had a swelling value of 4.85 ± 0.03%−5.45 ± 0.01%. This value is lower than the swelling value of MSGPvA, which is 9.92 ± 0.02%−10.72 ± 0.03% (Harsojuwono et al., 2021). However, the swelling value of all MSGPvA BtC with PCL and AMA did not meet the International Bioplastic Standard (EN 317), which stipulates a maximum swelling value of 1.44%. According to Ghavimi et al. (2014) and Lin and Razali (2019), mixing of PCL and polydimethylsiloxane (PDMS) will produce a composite with a hydrophobic–hydrophilic pattern, which affects the swelling properties and WVTR. Meanwhile, according to Aslam et al. (2018), different swelling characteristics between polymers are a result of different types and ratios of constituent materials, manufacturing processes, and chemical modifications carried out in the synthesis of new polymers. Chemical modification will change the chemical, physical, and mechanical properties if one of the main functional groups such as the hydroxyl group undergoes a reaction. Reactions that can occur include acetylation, etherification, esterification, and carbamation (Aslam et al., 2017). According to Harsojuwono and Arnata (2017), the hydroxyl group causes a compound to be polar, due to the electronegative oxygen atom being able to attract electrons. If the electrons come from water molecules, it will facilitate the dissolution of compounds containing the hydroxyl group.

Figure 5 shows that the MSGPvA BtC using 5% PCL and 0.5% AMA had the highest WVTR value (147.89 ± 2.03 g/m^2/day), which was not significantly different from the WVTR value of the MSGPvA BtC using 5% PCL with 1.5–3.5% AMA and 10% PCL with 0.5–2.5% AMA. Meanwhile, the MSGPvA BtC using 20%

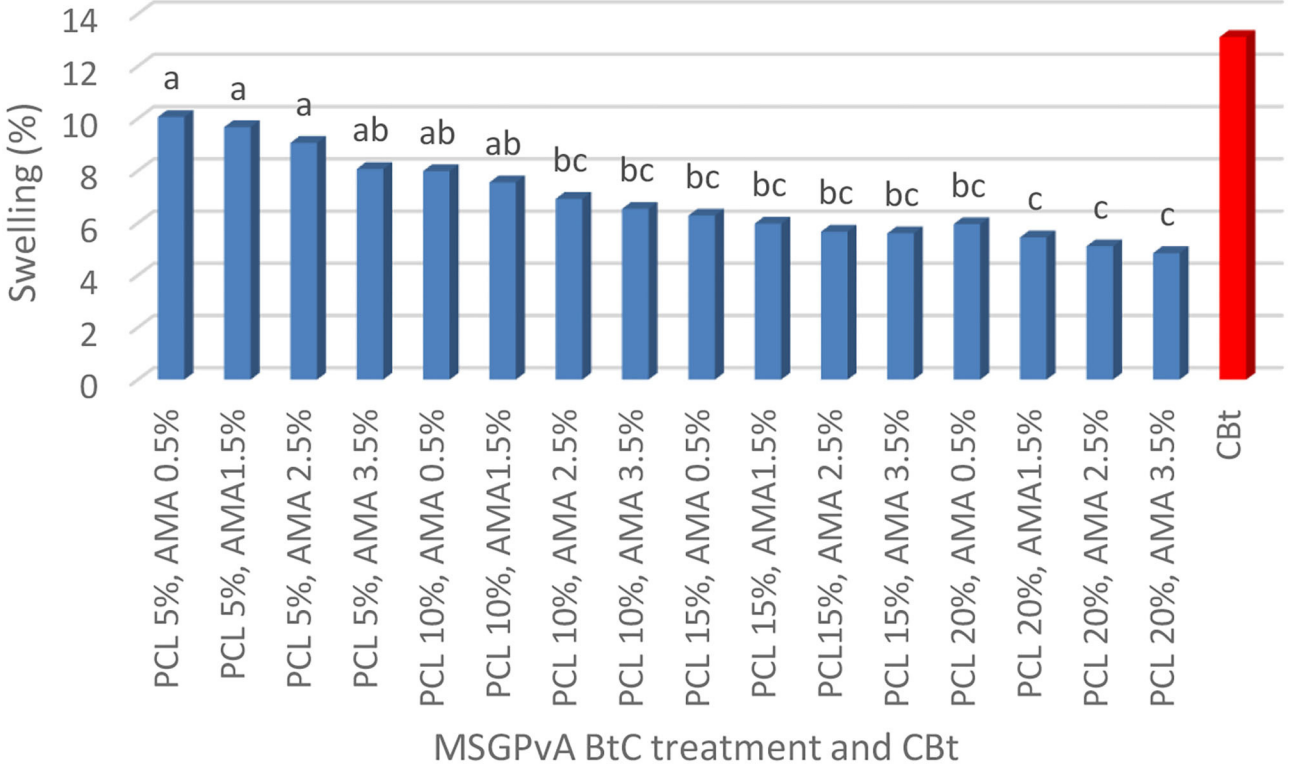

FIGURE 4 | Relationship of MSGPvA BtC and CBt with swelling.

PCL and 3.5% AMA had the lowest WVTR value (91.12 ± 1.13 g/m^2/day), which was not significantly different from the WVTR value of the MSGPvA BtC using 10% PCL and 3.5% AMA, 15% PCL and 0.5–3.5% AMA, and 20% PCL and 0.5–2.5% AMA.

The MSGPvA BtC with 20% PCL and 3.5% AMA had a WVTR value of 91.12 ± 1.13 g/m^2/day. This value is much lower than the WVTR of starch:carrageenan BtC (25:75) with 1.5–6.0% PCL, which has a WVTR value of 264.14 ± 3.33–272.46 ± 5.54 g/m^2/day (Hartiati et al., 2021). According to Murdinah et al. (2007), WVTR will decrease with increasing hydrophobicity. Meanwhile, according to Darni and Utami (2010), hydrophilic properties are characteristics of water-loving materials that affect WVTR. Ferreira et al. (2016) explained that the nature of WVTR is influenced by the constituent materials of a bioplastic composite so as to determine the ability of biocoating or biopackaging in influencing gas and water vapor exchange. The higher the WVTR value, the higher the water vapor permeability of a film as well.

Meanwhile, **Figure 6** shows that MSGPvA BtC using PCL and AMA had degradation times that were not significantly different in all concentration treatments with values ranging from 6.33 ± 0.11 to 7.67 ± 0.13 days. The MSGPvA BtC with PCL and AMA had a degradation time similar to that of MSGPvA ranging from 6.25 ± 0.09 to 6.50 ± 0.06 days (Harsojuwono et al., 2021). Both BtCs had biodegradation time values that were in accordance with ASTM 5336 for PLA from Japan and PCL from the UK, which set a maximum biodegradation time of 60 days.

Basically, biodegradation begins with chemical degradation, which is molecular oxidation which produces a smaller molecular weight and is followed by the attack of microorganisms that break it down into very simple molecules and minerals (Waryat et al., 2013, 2018). According to Kumar and Thakur (2017), biopolymer degradation will produce simple compounds such as CO_2 and H_2O.

Surface Profile

The cross-sectional surface profile of the MSGPvA BtC with PCL and AMA is shown in **Figure 7A**. Meanwhile, a comparison with MSGPvA BtC from Harsojuwono et al. (2021) is shown in **Figure 7B**, and a comparison with the starch:carrageenan BtC (25:75) with 1% glycerol and 6% PVA from Hartiati et al. (2021) is shown in **Figure 7C**.

The cross-sectional surface profile of the MSGPvA BtC with PCL and AMA showed the presence of clear and wavy fibers. This is in contrast to MSGPvA, which did not reveal any obvious pores and fibers (Harsojuwono et al., 2021). The surface profile also differs from the cross-sectional surface profile of the starch:carrageenan BtC (25:75) with 1% glycerol and 6% PVA, indicating the presence of sloping peaks and troughs and layers of varying sizes (Hartiati et al., 2021). This explains that the MSGPvA BtC with PCL and AMA has a better cross-sectional surface profile than the MSGPvA BtC and starch:carrageenan BtC (25:75) with 1% glycerol and 6% PVA. According to

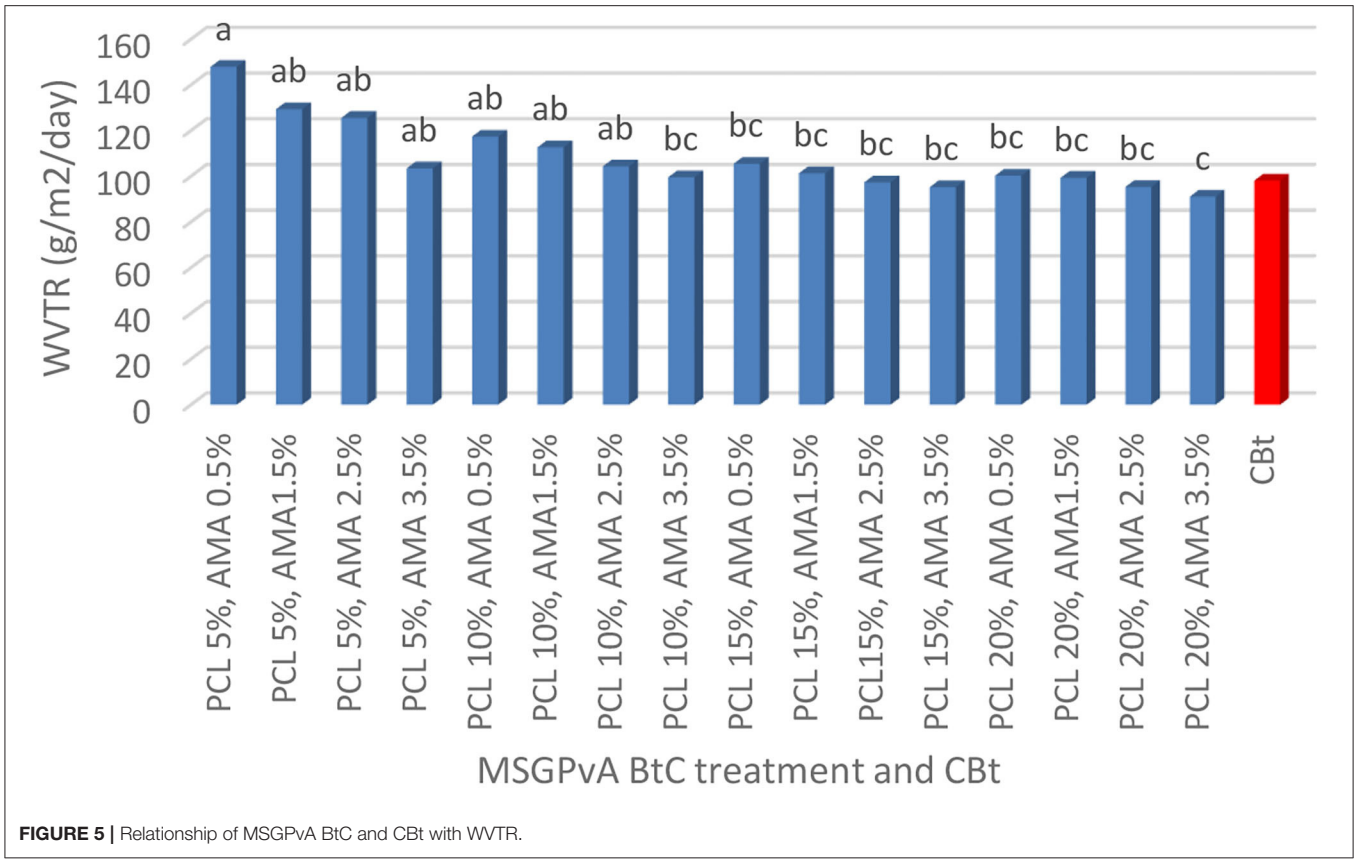

FIGURE 5 | Relationship of MSGPvA BtC and CBt with WVTR.

Camacho et al. (2011), the smooth and layered surface protrusion is due to the linear orientation of the polymer.

The longitudinal surface profile of the MSGPvA BtC with PCL and AMA is shown in **Figure 7D**. Meanwhile, a comparison with MSGPvA BtC from Harsojuwono et al. (2021) is shown in **Figure 7E**, and a comparison with the starch:carrageenan BtC (25:75) with 1% glycerol and 6% PVA from Hartiati et al. (2021) is shown in **Figure 7F**.

The longitudinal surface profile of the MSGPvA BtC with PCL and AMA showed a smooth surface with indistinct waves. This is in contrast to the longitudinal surface profile of MSGPvA, which showed a clearer wave but did not reveal the presence of fibers or pores (Harsojuwono et al., 2021). The longitudinal surface profile is also very different from the longitudinal surface profile of the starch:carrageenan BtC (25:75) with 1% glycerol and 6% PVA, which indicates the presence of evenly distributed small block-shaped granules with few pores between the granules (Hartiati et al., 2021). This explains that the MSGPvA BtC with PCL and AMA has a better longitudinal surface profile than the MSGPvA BtC and starch:carrageenan BtC (25:75) with 1% glycerol and 6% PVA.

Functional Groups

The components that make up the BtC greatly affect the type of functional groups contained in the material. **Figure 8A** shows the wavenumber of the spectrogram of the MSGPvA BtC with PCL and AMA, while **Figure 8B** shows the spectrogram wavenumber of MSGPvA BtC from Harsojuwono et al. (2021). Meanwhile, **Table 1** shows the functional groups in the wavenumber.

The functional groups contained in the MSGPvA BtC with PCL and AMA include O-H at wavenumbers 2,962.66 and 3,448.72 cm^{-1} and C=O at wavenumber 1,735.93 cm^{-1}. This is slightly different when compared to the functional groups contained in the MSGPvA BtC, which contains a functional group (O-H) at wavenumbers 2,140.99 and 3,360.89 cm^{-1}: C-H at wavenumber 1,712.79 cm^{-1}, C-O at wavenumber 1,188.15 cm^{-1}, and (–(CH_2)n) at wavenumber 435.91 cm^{-1} (Harsojuwono et al., 2021). This indicates a change in the functional group and a shift in the wavenumber of the MSGPvA BtC if the MSGPvA BtC is added with PCL and AMA. Alias et al. (2018) explained that the formation of a composite film from a polymer with PVA caused a shift in the wavenumber of the hydroxyl group of PVA from 3,279.10 to 3,278.67 and 3,260.93 cm^{-1}.

According to Perez and Francois (2016), changes in intensity and shift in wavenumber indicate good biocompatibility between biopolymers. Meanwhile, according to Ren et al. (2017), the shift in the functional groups of each polymer that makes up the BtC causes the formation of new bonds so that it changes the structure of the BtC with new characteristics. According to Dasbada (2015), although organic compounds have the same basic element, namely, carbon, they have very different properties from one another due to the different functional groups attached.

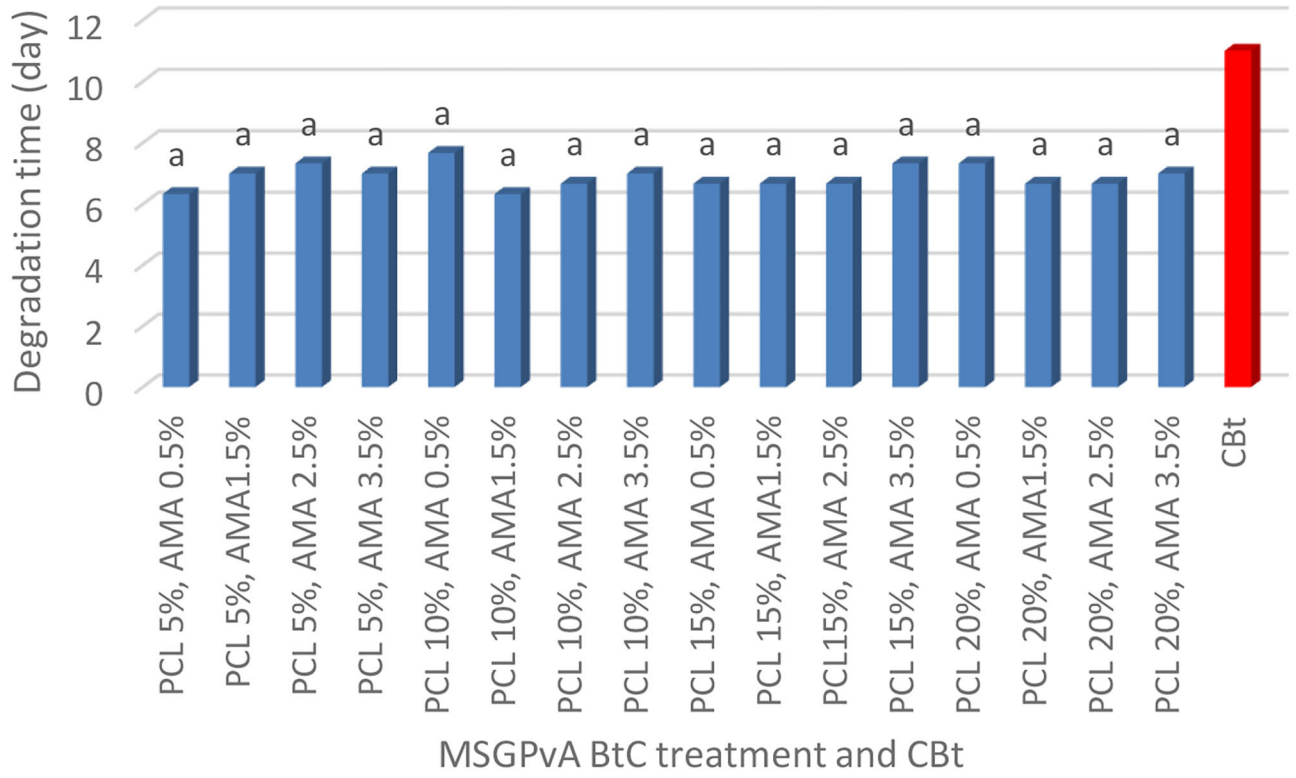

FIGURE 6 | Relationship of MSGPvA BtC and CBt with degradation time.

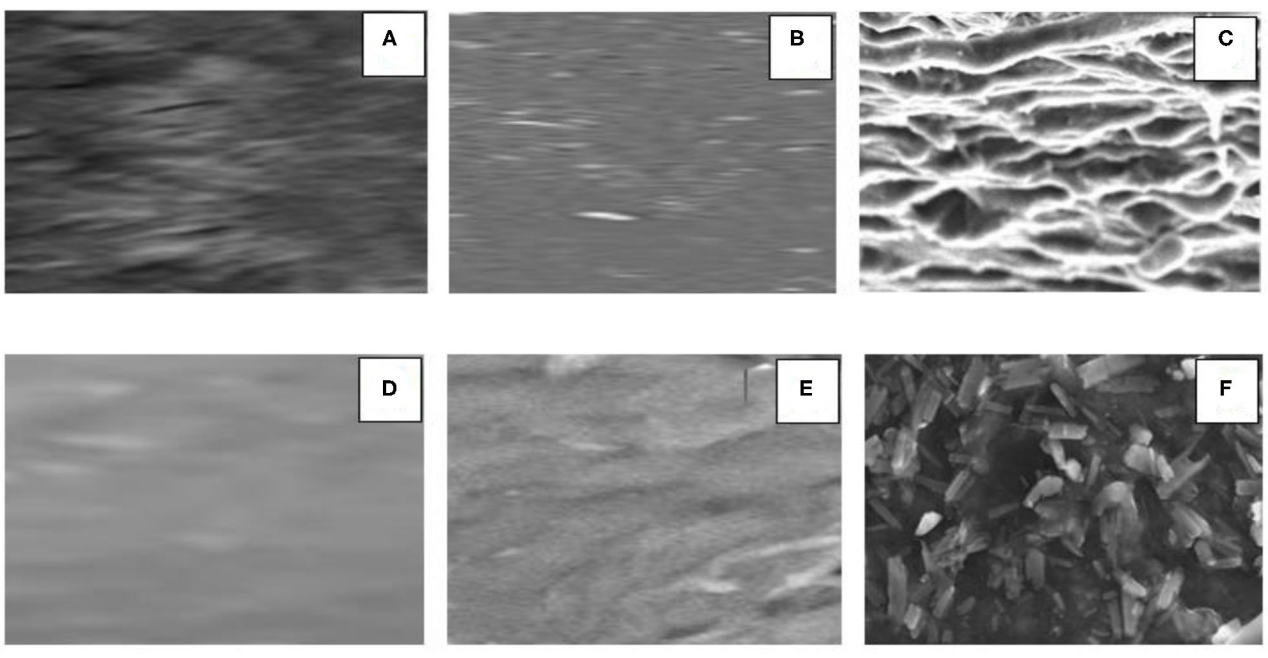

FIGURE 7 | Cross-sectional view of the surface profile of a BtC: **(A)** MSGPvA with PCL and AMA, **(B)** MSGPvA from Harsojuwono et al. (2021), and **(C)** the starch:carrageenan (25:75) with 1% glycerol and 6% PVA from Hartiati et al. (2021); longitudinal surface profile of **(D)** MSGPvA with PCL and AMA, **(E)** MSGPvA from Harsojuwono et al. (2021), and **(F)** the starch:carrageenan (25:75) with 1% glycerol and 6% PVA from Hartiati et al. (2021). All images with ×1,000 magnification.

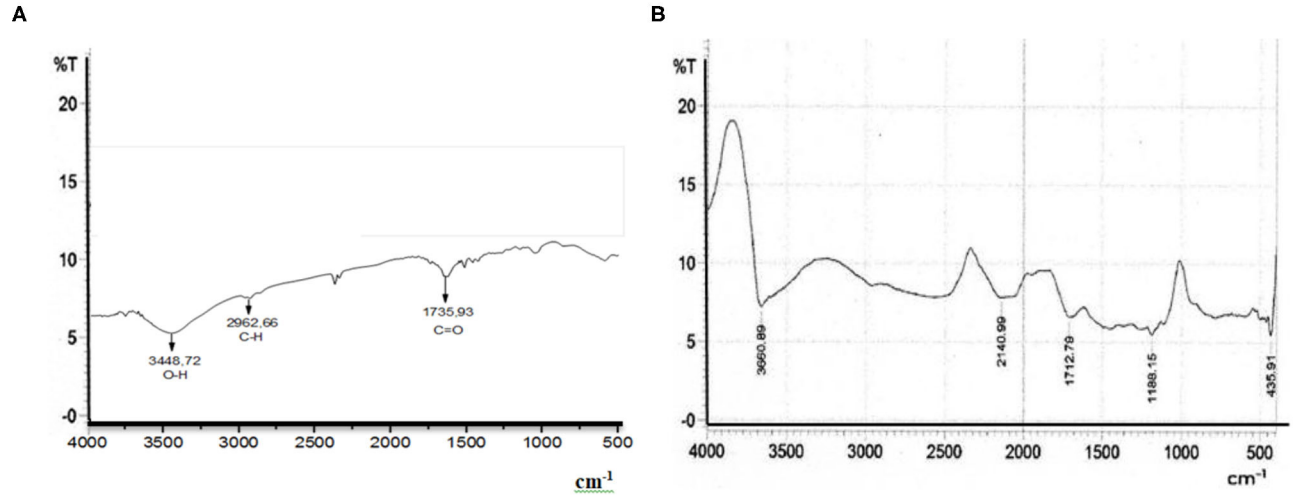

FIGURE 8 | Wavenumber spectra of BtC **(A)** MSGPvA with PCL and AMA **(B)** MSGPvA (Harsojuwono et al., 2021).

TABLE 1 | Wavenumbers and functional groups in MSGPvA BtC with PCL and AMA and MSGPvA BtC (Harsojuwono et al., 2021).

Standard wavenumber region (cm^{-1}) (Gable, 2014)	Standard functional group (Gable, 2014)	Wavenumber of MSGPvA BtC with PCL and AMA (cm^{-1})	Functional groups in MSGPvA BtC with PCL and AMA	Wavenumber of MSGPvA. BtC (cm^{-1}) (Harsojuwono et al., 2021)	Functional groups in MSGPvA BtC (Harsojuwono et al., 2021)
2,000–3,600	O-H alcohol	2,962.66, 3,448.72	O-H alcohol	2,140.99, 3,360.89	O-H alcohol
1,690–1,760	C=O	1,735.93	C=O	1,712.79	C=O
1,080–1,300	C-O			1,188.15	C-O
650–1,000	C-H			435.91	$(CH_2)_n$
<722	$(CH_2)_n$				

Degree of Crystallinity

The relationship between 2θ angle and X-ray diffraction intensity on MSGPvA BtC with and without PCL and AMA is presented in **Figure 9**. **Figure 9** shows that MSGPvA BtC with PCL and AMA has a lower diffraction intensity than MSGPvA BtC. Under these conditions, the MSGPvA BtC with PCL and AMA had a crystallinity degree of 20.80% with 2θ diffraction peaks located at 13.4°, 15.1°, 16.7°, 17.4°, 22.7°, and 29.3°, while MSGPvA BtC without PCL and AMA has a crystallinity degree of 71.64%.

The MSGPvA BtC with PCL and AMA had a lower crystallinity degree when compared to the MSGPvA BtC (Harsojuwono et al., 2021). According to Harsojuwono et al. (2021), the higher the intensity and density of the 2θ angle of X-ray diffraction, the higher the crystallinity degree. The sharp peaks at 2θ diffraction angles 6.7°, 7.2°, 14.5°, 19.5°, 20.5°, and 22.7° indicate that these materials have a crystalline structure (Yusuf et al., 2019).

The crystallinity degree of the MSGPvA BtC with PCL and AMA decreased more sharply than that of the MSGPvA BtC. This is due to the decreasing intensity and shifting of the diffraction peaks from the crystalline region to the more widespread amorphous region. This condition occurs because intermolecular and intramolecular hydrogen bonds are broken during the composite formation process, resulting in damage to the crystal structure of the constituent polymers (Yang et al., 2016). This is in accordance with the opinion of Zhang et al. (2018) who explained that in the composite system, there is a strong interaction of the polymeric materials that make up the composite. This causes the polymer to be easily dispersed even in the absence of a solvent (Altaani et al., 2020).

Thermal Stability

The thermal stability of the MSGPvA BtC with PCL and AMA is presented in **Figure 10**. **Figure 10A** shows the relationship between temperature and weight loss of the MSGPvA BtC with and without PCL and AMA. **Figure 10A** shows that the evaporation process in phase I took place up to a temperature of 100°C. Here, it can be seen that the MSGPvA BtC with PCL and AMA experienced a greater weight loss than the MSGPvA BtC. Furthermore, phase II is a physicochemical degradation process that occurs above 100°C. Meanwhile, **Figure 4B** shows the derivative of thermogravimetry (DTG) of the MSGPvA BtC with and without PCL and AMA. **Figure 10B** shows that the MSGPvA BtC with PCL and AMA has a higher weight loss rate than the MSGPvA BtC.

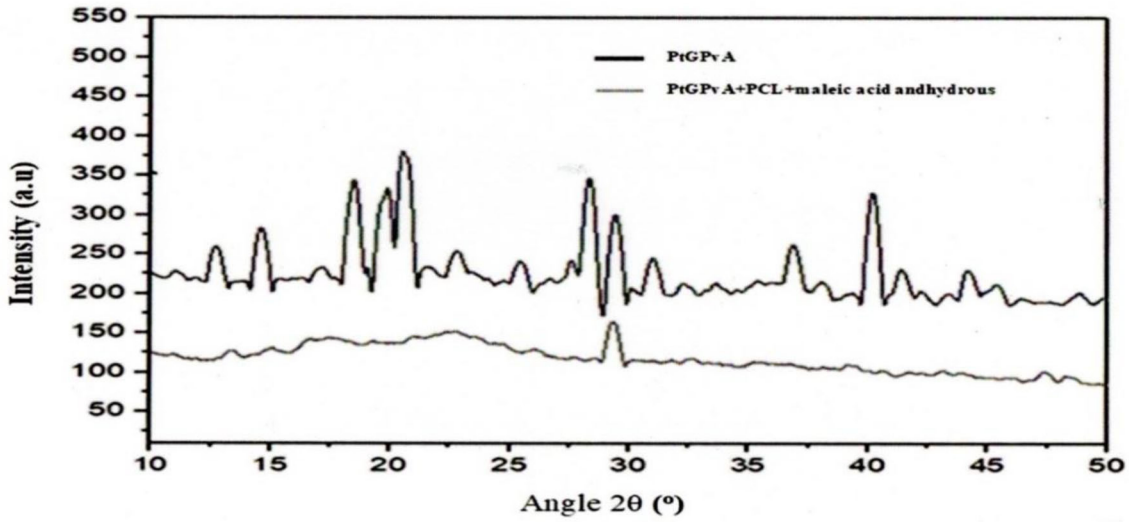

FIGURE 9 | Relationship between 2θ angle and X-ray diffraction intensity of MSGPvA BtC with and without PCL and AMA.

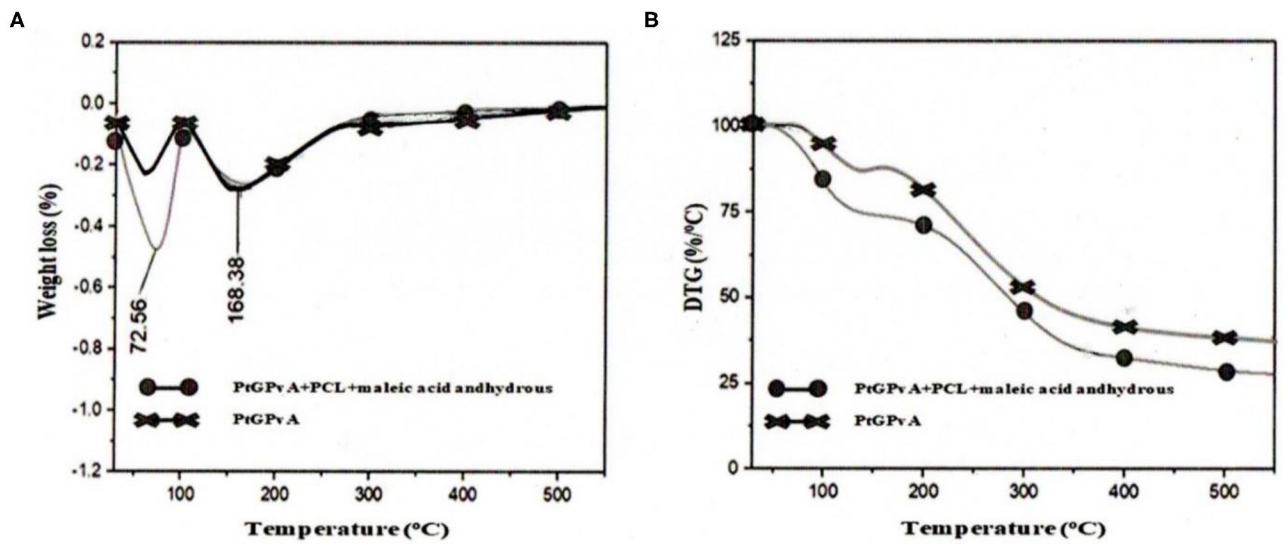

FIGURE 10 | Relationship between temperature with **(A)** weight loss **(B)** derivative of thermogravimetry of MSGPvA BtC with and without PCL and AMA.

Table 2 shows that the initial temperature of the evaporation process (phase I) of MSGPvA BtC with and without PCL and AMA is in the range of 37.99–43.31°C. The MSGPvA BtC with PCL and AMA had a maximum evaporation process temperature (72.56°C) which was lower than the maximum evaporation process temperature (78.43°C) from the MSGPvA BtC. This has an impact on the weight loss (4.73%) of the MSGPvA BtC with PCL and AMA, which is much greater than the weight loss (0.92%) of the MSGPvA BtC.

Table 2 also shows that the initial temperature of degradation of the MSGPvA BtC with PCL and AMA occurred at an initial temperature of 104.79°C, which was higher than the initial degradation temperature (101.84°C) of MSGPvA BtC. As a result, the maximum degradation temperature (221.01°C) of the MSGPvA BtC with PCL and AMA was also much higher than the maximum degradation temperature (168.38°C) of the MSGPvA BtC. The impact is that the MSGPvA BtC with PCL and AMA has a higher weight loss (30.15%) than the weight loss (9.20%) of the MSGPvA BtC, but on the other hand, the remaining charcoal is lower, which is 27.88 and 36.92%, respectively.

The thermal stability of a material is known from the ability of the material to survive in the evaporation process (phase I) and degradation (phase 2) (Perez and Francois, 2016). This process also occurs in the MSGPvA BtC with PCL and AMA. Phase I is a physical degradation, namely, the process of evaporation of free water from the material, which takes place up to a temperature

TABLE 2 | Initial temperature, maximum temperature, and weight loss in the evaporation process (phase I) and degradation (phase II) of MSGPvA BtC with and without PCL and AMA.

Material type	Phase I			Phase II			Remaining charcoal on 500°C (%)
	$T_{initial}$ (°C)	T_{max} (°C)	Weight losses on T_{max} (%)	$T_{initial}$ (°C)	T_{max} (°C)	Weight losses on T_{max} (%)	
MSGPvA	43.31	78.43	0.92	101.84	168.38	9.20	36.92
MSGPvA + PCL + AMA	37.99	72.56	4.73	104.79	221.01	30.15	27.88

of 100°C. In phase I, the shrinkage of the MSGPvA BtC with PCL and AMA was higher than the weight loss of the MSGPvA BtC. Meanwhile, the maximum evaporation temperature of the MSGPvA BtC with PCL and AMA was lower than that of the MSGPvA BtC. As a result, the weight loss of the MSGPvA BtC with PCL and AMA was much greater than that of the MSGPvA BtC, which reached 4.73%.

Phase II is a combination of physical and chemical degradation such as dehydration, decomposition, and depolymerization, which slims down at temperatures above 100°C (Arnata et al., 2020). Here, weight loss occurs, which is a complex process involving dehydration of the pyranose ring, depolymerization, and decomposition of glucose from starch (Fang et al., 2002). The largest weight loss occurred at a temperature of 200–400°C and tended to be stable in the temperature range of 350–550°C. Thermal properties in this temperature range are shown by the MSGPvA BtC with PCL and AMA.

The maximum degradation temperature of MSGPvA BtC with PCL and AMA occurred at 221.01°C. This temperature is much higher than the maximum degradation temperature for MSGPvA BtC (Harsojuwono et al., 2021). This had an impact on the weight loss of the MSGPvA BtC with PCL and AMA, which reached 30.15%. Meanwhile, the weight loss rate of the MSGPvA BtC with PCL and AMA was higher than that of the MSGPvA BtC at a temperature of around 72.56°C. However, the weight loss rate was stable for the two BtCs at temperatures above 350°C. The composing stage of the MSGPvA BtC with PCL and AMA occurred at a temperature of 500°C with a charcoal residue of 27.88%. The charcoal residue is formed due to the carbonation or pyrolysis process of polysaccharide and composite materials (Zawadzki and Kaczmarek, 2010). Further, the thermal degradation causes an oxidation process and the decomposition of charcoal residue into gaseous products with lower molecular weights (Silvério et al., 2013).

CONCLUSION

The concentration of PCL and AMA and their interactions had a very significant effect on elongation at break, the ratio of tensile strength and Young's modulus of MSGPvA BtC to CBt, swelling, and WVTR but had no effect on the degradation time of MSGPvA BtC. The MSGPvA BtC with 20% PCL and 3.5% AMA had the best characteristics with a ratio of 1.2 ± 0.01 for tensile strength, elongation at break of 8.01 ± 0.01%, ratio of 1.36 ± 0.01 for Young's modulus, swelling of 4.85 ± 0.03 %, WVTR of 91.12 ± 0.81 g/m^2/day, and degradation time of 7 ± 0.09 days.

The MSGPvA BtC with 20% PCL and 3.5% AMA had a transverse surface profile showing the presence of clear and wavy fibers and a longitudinal surface profile with indistinct waves, containing the OH functional group at wavenumbers 2,962.66 and 3,448.72 cm^{-1} and C=O at wavenumber 1,735.93 cm^{-1}, a crystalline degree of 20.80%, a maximum evaporation process temperature of 72.56°C, a maximum degradation temperature of 221.01°C, and a weight loss of 30.15%. All characteristics of the MSGPvA BtC with 20% PCL and 3.5% AMA, except swelling, have met the SNI and International Bioplastic Standards.

DATA AVAILABILITY STATEMENT

The datasets presented in this article are not readily available because the data listed in the article is data resulting from the measurement of variables carried out by the researcher/author himself. Requests to access the datasets should be directed to bambang.admadi@unud.ac.id.

AUTHOR CONTRIBUTIONS

BH planned, designed, and carried out the research. IA and AH carried out research and reports. YS and SH analyzed the data. LS created and translated the article. All authors contributed to the article and approved the submitted version.

FUNDING

The authors would like to thank Udayana University for providing financial support in the form of grants for the research, writing, and publication of this article.

REFERENCES

Abdurrozag, M. (2016). *Synthesis and Characterization of Biodegradable Plastic from a Mixture of Glucomannan Porang (Amorphophallus oncophillus PR.) and Cassava Starch (Manihot esculenta) with Glycerol as Plasticizer*. Available online at: http://lib.unnes.ac.id/26913/ (accessed November 2, 2020).

Akbari, B., and Bagheri, R. (2012). Influence of compatibilizer and processing conditions on morphology, mechanical properties, and

deformation mechanism of PP/Clay nanocomposite. *J. Nanomat*. 10, 1–18. doi: 10.1155/2012/810623

Alias, N. F., Ismail, H., Wahab, M. K. A., Ragunathan, S., Ardhyananta, H, and Ting, S. S. (2018). Development of new material based on polyvinyl alcohol/palm kernel shell powder biocomposites. *Adv. Env. Stud*. 2, 98–107. doi: 10.36959/742/208

Altaani, B., Obaidat, R., and Malkawi, W. (2020). Enhancement of dissolution of atorvastatin through preparation of polymeric solid dispersions using supercritical fluid technology. *Res. Pharm. Sci*. 15, 123–136. doi: 10.4103/1735-5362.283812

Anonymous (2020). *Polycaprolactone*. Availbale online at: http://en.jurenhg.com/product/1.html (accessed November 5, 2020).

Arnata, I. W., Suprihatin, S., Fahma, F, and Richana, N. (2020). Cationic modification of nanocrystalline cellulose from sago fronds. *Cellulose*. 27, 3121–3141. doi: 10.1007/s10570-019-02955-3

Aslam, M., Kalyar, M. A., and Raza, Z. A. (2017). Graphene oxides nanosheets mediation of poly(vinyl alcohol) films in tuning their structural and opto-mechanical attributes. *J. Mat. Sci. Mat. Elec*. 28, 13401–13413 doi: 10.1007/s10854-017-7177-y

Aslam, M., Kalyar, M. A., and Raza, Z. A. (2018). Polyvinyl alcohol: a review of research status and use of polyvinyl alcohol based nanocomposites. *Pol. Eng. Sci*. 58, 2119–2132. doi: 10.1002/pen.24855

Averous, L. (2007). Biodegradable multiphase system based on plasticized starch: a review. J. *Macromol. Sci*. 44, 231–274. doi: 10.1081/MC-200029326

Camacho, D. H., Tambio, S. J. M., and Oliveros, M. I. A. (2011). Carrageenan-ionic liquid composite: development of polysaccharide-based solid electrolyte system. *Manila J. Sci*. 6, 8–15. Available online at: https://www.dlsu.edu.ph/wp-content/uploads/pdf/research/journals/mjs/MJS06-2-2011/MJS06-2-2-camacho.pdf

Carballo, Z. B. C., Aranda, S. D., and Escamilla, G. C. (2017). Properties and biodegradability of thermoplastic starch obtained from granular starches grafted with polycaprolactone. *Int. J. Pol. Sci*. 2017:3975692. doi: 10.1155/2017/3975692

Chen, B., and Sun, K. (2005). Poly(caprolactone)/hydroxyapatite composites effects of particle size, molecular weight distribution and irradiation on interfacial interaction and properties. *J. Pol. Test*. 24, 64–70. doi: 10.1016/j.polymertesting.2004.07.010

Darni, Y., and Utami, A. (2010). "Synthesis of bioplastics from banana starch and gelatin with glycerol as plasticizer," in: *Proceedings of the National Seminar on Science and Technology-II*. Lampung: University of Lampung.

Dasbada, F. (2015). *Functional Groups of Carbon Compounds*. Available online at: https://about-kimia.blogspot.com/2015/10/gugus-function-elektron-carbon.html (accessed January 6, 2021).

Dewi, G. A. A. M. P., Harsojuwono, B. A., and Arnata, I. W. (2015). Effect of composite material mixture and glycerol concentration on bioplastic characteristics of cassava peel starch. *J. Agroin. Eng. Manag*. 3, 41–50. Available online at: https://ojs.unud.ac.id/index.php/jtip/article/view/18810

Dome, K., Podgorbunskikh, E., Bychkov, A, and Lomovsky, O. (2020). Changes in the crystallinity degree of starch having different types of crystal structure after mechanical pretreatment. *Polymers*. 12, 1–12. doi: 10.3390/polym12030641

Fang, J., Fowler, P. A., Tomkinson, J, and Hills, C. A. S. (2002). The preparation and characterization of a series of chemically modified potato starches. *Carb. Pol*. 47, 245–252. doi: 10.1016/S0144-8617(01)00187-4

Ferreira, A. R. V., Alves, V. D., and Coelhoso, I. M. (2016). Polysaccharide-based membranes in food packaging applications. *Membranes*. 6, 22–42. doi: 10.3390/membranes6020022

Firdaus, F., and Anwar, C. (2014). Potential liquid solid waste of tapioca flour industry as raw material for biodegradable plastic films. *J. Logic*. 1, 14–21. Available online at: https://journal.uii.ac.id/Logika/article/view/458

Frost, K., Kaminski, D., Kirwan, G., Lascaris, E., and Shanks, R. (2009). Crystallinity and structure of starch using wide angle X-Ray scattering. *Carb. Pol*. 78, 543–548. doi: 10.1016/j.carbpol.2009.05.018

Gable, K. P. (2014). *Infrared Spectroscopy: Identifying Functional Groups*. Oregon State University. Available online at: https://www.science.oregonstate.edu/~gablek/CH335/Chapter10/IR.htm (accessed November 2, 2020).

Ghavimi, S. A. A., Ebrahimzadeh, M. H., Solati-Hashjin, M., and Osman, N. A. A. (2014). Polycaprolactone/starch composite: fabrication, structure, properties, and applications. *J. Biomed. Mat. Res*. 103, 2482–98. doi: 10.1002/jbm.a.35371

Harsojuwono, B. A., and Arnata, I. W. (2016). Physical and mechanical characteristics of bioplastics (Study of tapioca concentration and comparison of plasticizer mixtures). *Food Tech. Sci. Med*. 3, 1–7. Available online at: https://ojs.unud.ac.id/index.php/pangan/article/view/23155

Harsojuwono, B. A., and Arnata, I. W. (2017). Agricultural industrial polymer technology. *Intermedia. Malang. Indonesia*. 145–164.

Harsojuwono, B. A., Arnata, I. W., and Mulyani, S. (2017). Biodegradable plastic characteristics of cassava starch modified in variations temperature and drying time. *J. Chem. Proc. Eng. Res*. 49, 1–5.

Harsojuwono, B. A., Arnata, I. W., and Mulyani, S. (2018). Bio-plastic characteristics from cassava starch modified in variations the temperature and pH of gelatinization. *Res. J. Pharm. Bio. Chem. Sci*. 9, 290–296. Available online at: https://www.rjpbcs.com/2018_9.2.html

Harsojuwono, B. A., Hartiati, A., and Hatiningsih, S. (2021). Characteristics of the glucomannan - modified cassava starch biothermoplastic composites on the variety of types and concentrations of reinforcing materials. *Int. J. Pharm. Res*. 13, 912–923. doi: 10.31838/ijpr/2021.13.02.143

Harsojuwono, B. A., Mulyani, S., and Arnata, I. W. (2019). Characteristics of bio-plastic composites from the modified cassava starch and konjac glucomannan. *J. Appl. Hortic*. 21, 101–107. doi: 10.37855/jah.2019.v21i01.02

Harsojuwono, B. A., Mulyani, S., and Arnata, I. W. (2020). Bio-plastic composite characteristics of the modified cassava starch-glucomannan in variations of types and addition of fillers. *J. Appl. Hortic*. 22, 154–163. doi: 10.37855/jah.2020.v22i03.32

Hartiati, A., Harsojuwono, B. A., Suyanto, H., and Arnata, I. W. (2021). Characteristics of starch-based bioplastic composites in the ratio variations of the polysaccharide mixture. *Int. J. Pharm. Res*. 13, 1500–1512. doi: 10.31838/ijpr/2021.13.02.223

Hestuti, E., Komar, S., and Sutriah, M. (2017). Palm oil-based surfactants for enhanced oil recovery (EOR) applications in the intermediate oil field. *Oil Gas Pub. Sheet*. 44, 108–116. Available online at: http://journal.lemigas.esdm.go.id/index.php/LPMGB/article/view/10

Kumar, S., and Thakur, K. S. (2017). Review paper: bioplastic-classification, production and their potential food aplications. *J. Hill Agric*. 8, 118–129. doi: 10.5958/2230-7338.2017.00024.6

Lin, W. C., and Razali, N. A. M. (2019). Temporary wettability tuning of pcl/pdms micropattern using the plasma treatments. *Materials* 12, 1–16. doi: 10.3390/ma12040644

Melani, A., Herawati, N., and Kurniawan, A. F. (2017). Bioplastics of taro tuber starch through the melt intercalation process (study on the effect of filler type, filler concentration and type of plasticizer). *J. Dist*. 2, 53–67. doi: 10.32502/jd.v2i2.1204

Muin, H. (2019). "Copolymerization of lldpe with maleic anhydride without initiator in laboplastomyl," in *Proceedings of the National Symposium on Polymers*, V. Bandung, 65–70.

Murdinah, M., Darmawan, M., and Fransiska, D. (2007). Characteristics of edible films from alginate, gluten and beeswax composites. *J. Postharv. Mar. Fish. Biotech*. 2, 19–25. doi: 10.15578/jpbkp.v2i1.30

Nayiroh, N. (2013). *Composite Material Technology*. Available online at: http://nurun.lecturer.uin-malang.ac.id/wp-content/uploads/sites/7/2013/03/material-komposit.pdf (accessed June 25, 2021).

Perez, J. J., and Francois, N. J. (2016). Chitosan-starch bead prepared by ionotropic gelation as potential matrices for controlled release of fertilizers. *Carb. Pol*. 148, 134–142. doi: 10.1016/j.carbpol.2016.04.054

Prachayawarakorn, J., Sangnitidej, P., and Boonpasith, P. (2010). Properties of thermoplastic rice starch composites reinforced by cotton fiber or low-density polyethylene. *Carb. Pol*. 81, 425–433 doi: 10.1016/j.carbpol.2010.02.041

Pushpadass, H. A., Robert, W. W., Joseph, J. D., and Milford, A. H. (2010). Biodegradation characteristics of starch–polystyrene loose-fill foams. In a composting medium. *Biores. Techno*. 101, 7258–7264.doi: 10.1016/j.biortech.2010.04.039

Ren, L., Yan, X., and Zhou, J. (2017). Influence of chitosan concentrasion on mechanical and barrier properties of corn starch/chitosan films. *Int. J. Biol. Macromol*. 105, 1636–1643. doi: 10.1016/j.ijbiomac.2017.02.008

Ryden, E., Larsson, M., Zeliner, L, and Kleshchanok, D. (2016). *Biodegradable Polycaprolactone as a Mechanical Property Enhancer for Bioplastics*. Availabel online at: https://lup.lub.lu.se/student-papers/search/publication/8520637 (accessed November 5, 2020).

Sharma, R., Bisen, D. P., Shukia, U., and Sharma, B. G. (2012). X-Ray diffraction: a powerful method of characterizing nanomaterials, Rec. *Res. Sci. Tech*. 4, 77–79. Available online at: https://updatepublishing.com/journal/index.php/rrst/article/view/933

Silvério, H. A., Neto, W. P. F., Dantas, N. O., and Pasquini, D. (2013). Extraction and characterization of cellulose nanocrystals from corncob for application as reinforcing agent in nanocomposites. *Ind. Crops and Prod*. 44, 427–436. doi: 10.1016/j.indcrop.2012.10.014

Tong, Z., Chen, Y., and, Liu, Y. (2017). Preparasion, characterization and properties of Alginate/Poly(γ-glutamic acid) composite microparticles. *Mar. Drugs*. 15, 1–14. doi: 10.3390/md15040091

Warastuti, Y., Suryani, N., and Suryani, N. S. (2017). Degradation characteristics of irradiated poly-(caprolactone-chitosan-hydroxyapatite) biomaterial in a simulated body fluid solution. *J. Isot. Rad. App*. 10, 11–22. Available online at: http://jurnal.batan.go.id/index.php/jair/article/download/1198/1143

Waryat, R. M., Suryani, A., Yuliasih, I., Johan S, and Nasiri, A. (2018). Utilization of thermoplastic starch as raw material for environmentally friendly plastic packaging. *Indo. J. Mat. Sci*. 14, 214–221. Available online at: https://adoc.pub/pemanfaatan-pati-termoplastik-sebagai-bahan-baku-plastik-kem.html

Waryat, R. M., Suryani, A., Yuliasih, I., and Johan, S. (2013). Characteristics of morphology, thermal, physical-mechanical, and barrier of biodegradable plastic made from LLDPE/HDPE thermoplastic starch composite. *J. Agritech*. 33, 197–207. doi: 10.22146/agritech.9800

Yang, L., Guo, J., Yu, Y., An, Q., Wang, L., Li, S., et al. (2016). Hydrogen bonds of sodium alginate/antarctic krill protein composite material. *J. Carb. Pol*. 142, 275–281. doi: 10.1016/j.carbpol.2016.01.050

Yusuf, H., Nugraheni, R. W., and Setyawan, D. (2019). Effect of cellulose derivative matrix and oligosaccharide on the solid state and physical characteristics of dimethyldioctadecylammoniumliposomes for vaccine. *Res. Pharm. Sci*. 14, 1–11. doi: 10.4103/1735-5362.251847

Zawadzki, J., and Kaczmarek, H. (2010). Thermaltreatment of chitosan in various conditions. *Carb. Pol*. 80, 394–400. doi: 10.1016/j.carbpol.2009.11.037

Zhang, R., Guo, Y., Liu, Y., Chen, S., Zhang, S, and Yu, Y. (2018). Effects of sodium salt types on the intermolecular interaction of sodium alginate/antarctic krill protein composite fibers. *Carb. Pol*. 189, 72–78. doi: 10.1016/j.carbpol.2018.02.013

Zhong, I. W., and Kang, F. C. (2008). Functional and smart materials structural evolution and structure analysis. New York, NY: Plenum Press, 76–86.

Conflict of Interest: The authors declare that the research was conducted in the absence of any commercial or financial relationships that could be construed as a potential conflict of interest.

Publisher's Note: All claims expressed in this article are solely those of the authors and do not necessarily represent those of their affiliated organizations, or those of the publisher, the editors and the reviewers. Any product that may be evaluated in this article, or claim that may be made by its manufacturer, is not guaranteed or endorsed by the publisher.